SUPPLEMENTAL INFORMATION

SUPPLEMENTAL FIGURE LEGENDS

Figure S1 (related to Figure 3): *blmp-1* Interaction with Precocious and Retarded Heterochronic Loci.

(A and B) Representative DIC images of L4 larvae or young adults (yA) showing alae formation in WT, precocious (*lin-42(n1089), lin-41i*) and retarded (*lin-29(n546), mab-10(e1248)*) mutants on L4440 empty vector control or upon *blmp-1* depletion, respectively. Scale bar = 10 μm. Arrowheads indicate seam cell positions, the origin of adult alae synthesis. **(C)** *blmp-1* knockdown increases the number of seam cells that undergo an extra division after the larval-to-adult transition in *mab-10(e1248)* mutants. The number of seam cells was scored in worms carrying 1-5 eggs using the *scm-1::gfp* marker. The number of theoretically present seam cells per side (16) was subtracted from the results to get the number of cells with extra divisions. ***p<0.001 (ANOVA). Mean+SD (n≥17).

Figure S2 (related to Figure 5): *blmp-1* Overexpression Enhances *dre-1* Phenotypes.

(A) *blmp-1* overexpression (OE) using an integrated *blmp-1::gfp* transgene (*wgIs109*, Sarov et al., 2012) induces gonadal migration defects in *dre-1* depleted worms. **p<0.01 (ANOVA). Mean+SEM (n=3, 40 gonadal arms each). **(B)** Micrographs of molting defects observed in *blmp-1* OE worms grown on *dre-1* RNAi. Scale bar = 10 μm. **(C)** Quantification of molting defects induced by *dre-1* depletion in *blmp-1* OE worms. **p<0.01 (ANOVA). Mean+SEM (n=3, 20 worms each).

Figure S3 (related to Figure 5): BLMP-1::GFP and NHR-25::GFP Overlap with DRE-1::GFP Expression, but only BLMP-1::GFP Depends on the SCF^{DRE-1} Complex.

(A) Representative DIC and fluorescence images showing overlapping expression patterns of DRE-1-, BLMP-1- and NHR-25::GFP in seam (se) and hypodermal (hyp) nuclei. **(B)** Representative fluorescence images showing BLMP-1::GFP intensity in seam and hypodermal nuclei upon various RNAi treatments. **(C)** NHR-25::GFP expression in seams varies with the molt cycle, but does not depend on *dre-1*. Each dot represents mean GFP intensity in >5 seam cells of a worm. Developmental age is given in hours (h) post-hatching. **(D)** His-DRE-1 co-precipitates with FLAG-HA-tagged (F/H) BLMP-1 when co-transfected in HEK293T cells treated with 15 μM MG132. F/H-RFP and -LIN-29 serve as negative controls.

Scale bars = 10 μm.

Figure S4 (related to Figure 6): DRE-1/FBXO11 Controls BLMP-1/BLIMP-1 Protein Turnover.

(A) Human His-BLIMP-1 co-precipitates with co-expressed F/H-FBXO11 from HEK293T cells only when treated with MG132. Detected protein sizes as in Figure 6C. **(B)** DRE-1 promotes BLMP-1 degradation via the proteasome. HEK293T cells were transfected with His-BLMP-1 and -LIN-29 in combination with F/H-DRE-1. Transfected cells were treated with cycloheximide (CHX) or CHX + MG132 for the indicated time intervals prior to harvesting and analysis by immunoblotting. **(C)** DN-CUL1(1-452) prevents FBXO11-dependent human BLIMP-1 degradation. HEK293T cells were transfected with His-BLIMP-1 and -RFP in combination with F/H-tagged FBXO11 ± FLAG-DN-CUL1. Transfected cells were treated with CHX for the indicated time intervals prior to harvesting and analysis by immunoblotting. Human BLIMP-1 stability was quantified from ≥3 independent experiments and normalized to co-expressed His-RFP. Mean+SD (n≥3). **(D)** Specifically DN-

CUL1(1-452), but not DN-CUL2(1-427) or DN-CUL3(1-418), stabilizes human BLIMP-1. Experimental setup as in (C).

Figure S5 (related to Figure 7): DRE-1::GFP in the Dtcs Increases with Age.

(A+B) Two independent integrated DRE-1::GFP lines (A and B) were analyzed. Developmental age is given in hours (h) post-hatching. Solid lines represent linear regression fits for illustration. In (A) each dot represents GFP intensity in one dtc. In (B) each dot represents mean GFP intensity of >5 seam cells of a worm.

Table S1 (related to Figure 1): *blmp-1(tm548)* Mutants do not Show Alterations in Seam Cell Number or Timing of the Seam Cell Fusion.

Seam cell fusion (*ajm-1:gfp* marker) and seam cell number (*scm-1::gfp* marker) were scored at the given stages. The number of animals scored is indicated in parentheses.

Table S2 (Excel file, related to Figure 7): Genes Regulated by the Transcription Factor *blmp-1*.

Gene list of significantly up- and downregulated genes (≥1.5-fold change, q-value<0.05) in *blmp-1(tm548)* mutant vs WT L3 larvae as obtained from RNA-sequencing analysis (n=3).

Figure S1 (related to Figure 3)

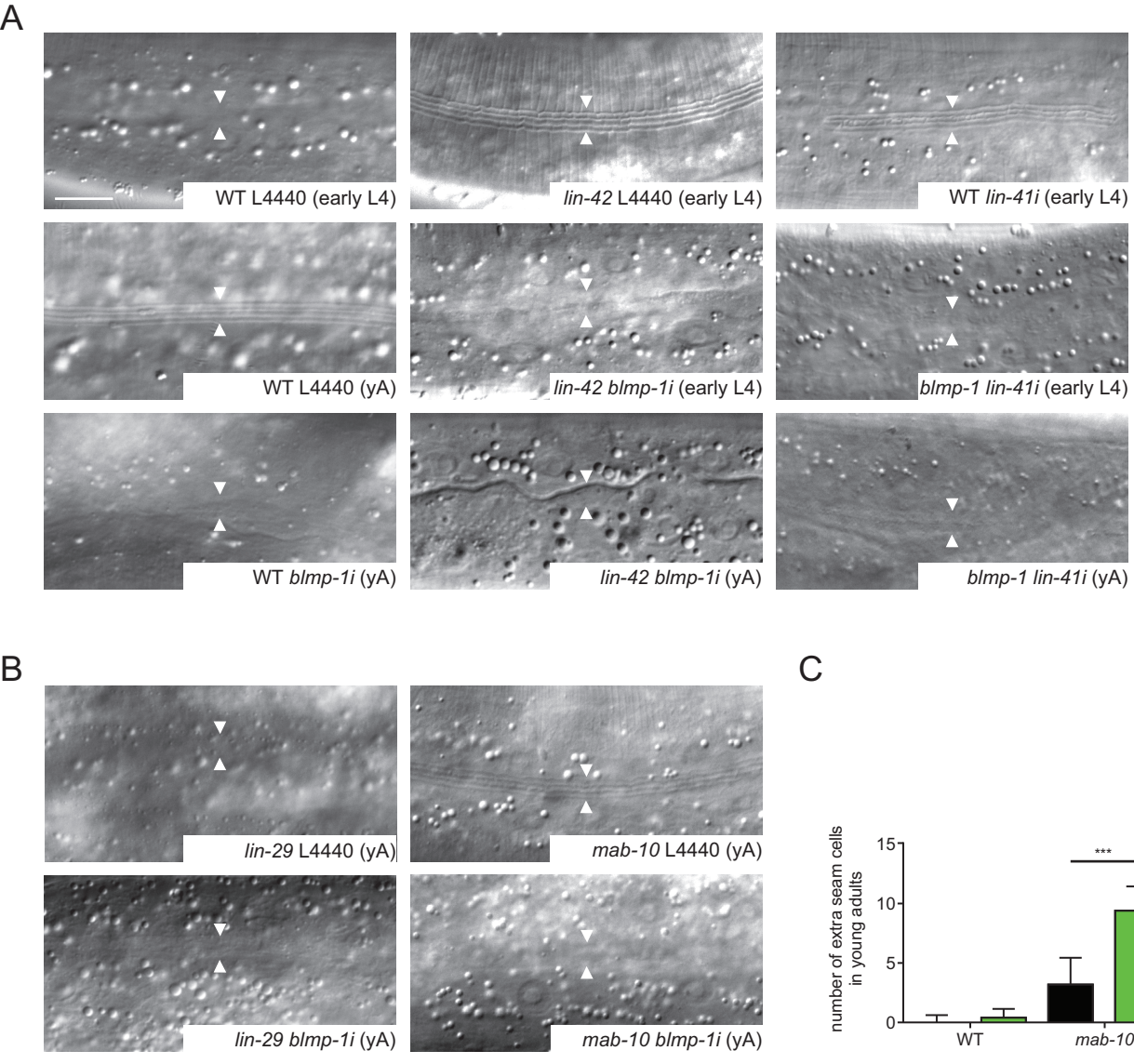

Figure S2 (related to Figure 5)

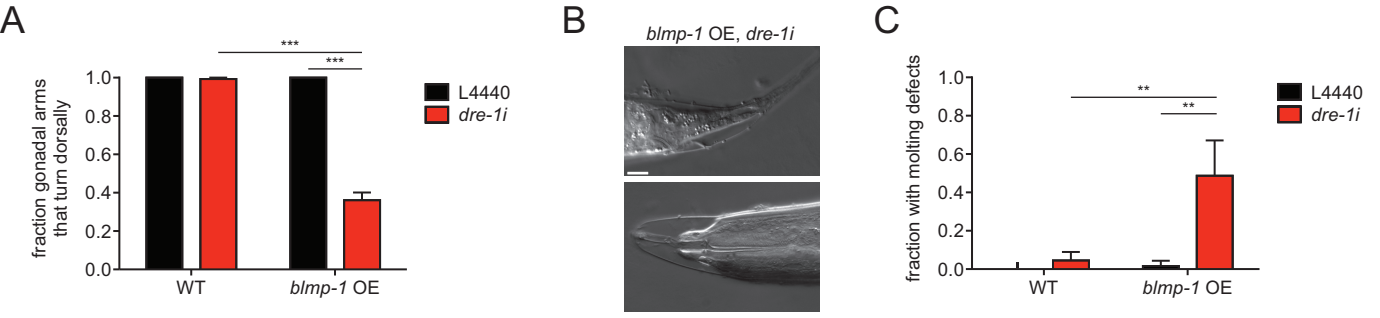

Figure S3 (related to Figure 5)

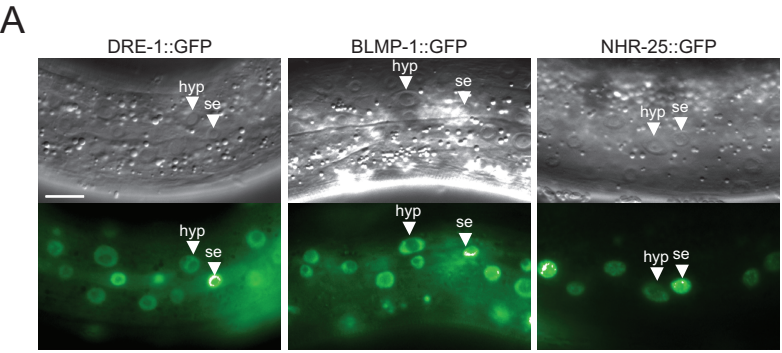

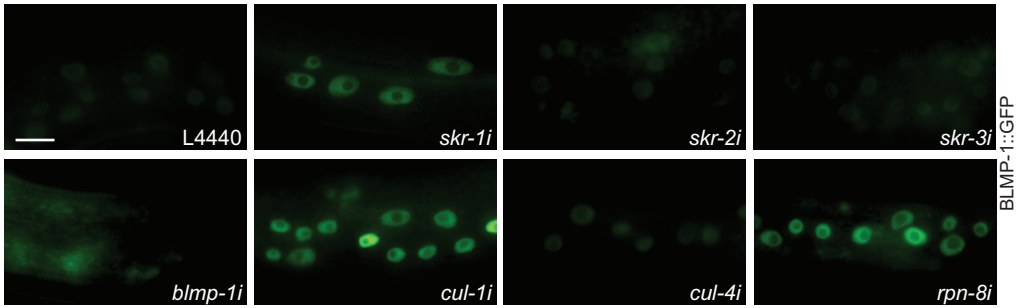

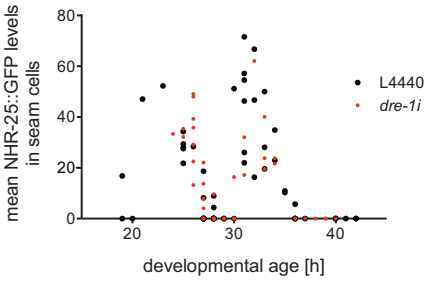

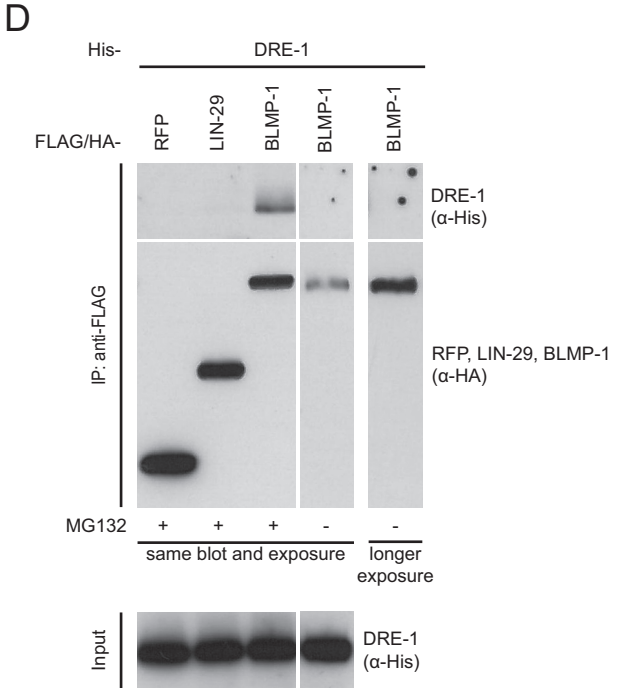

Figure S4 (related to Figure 6)

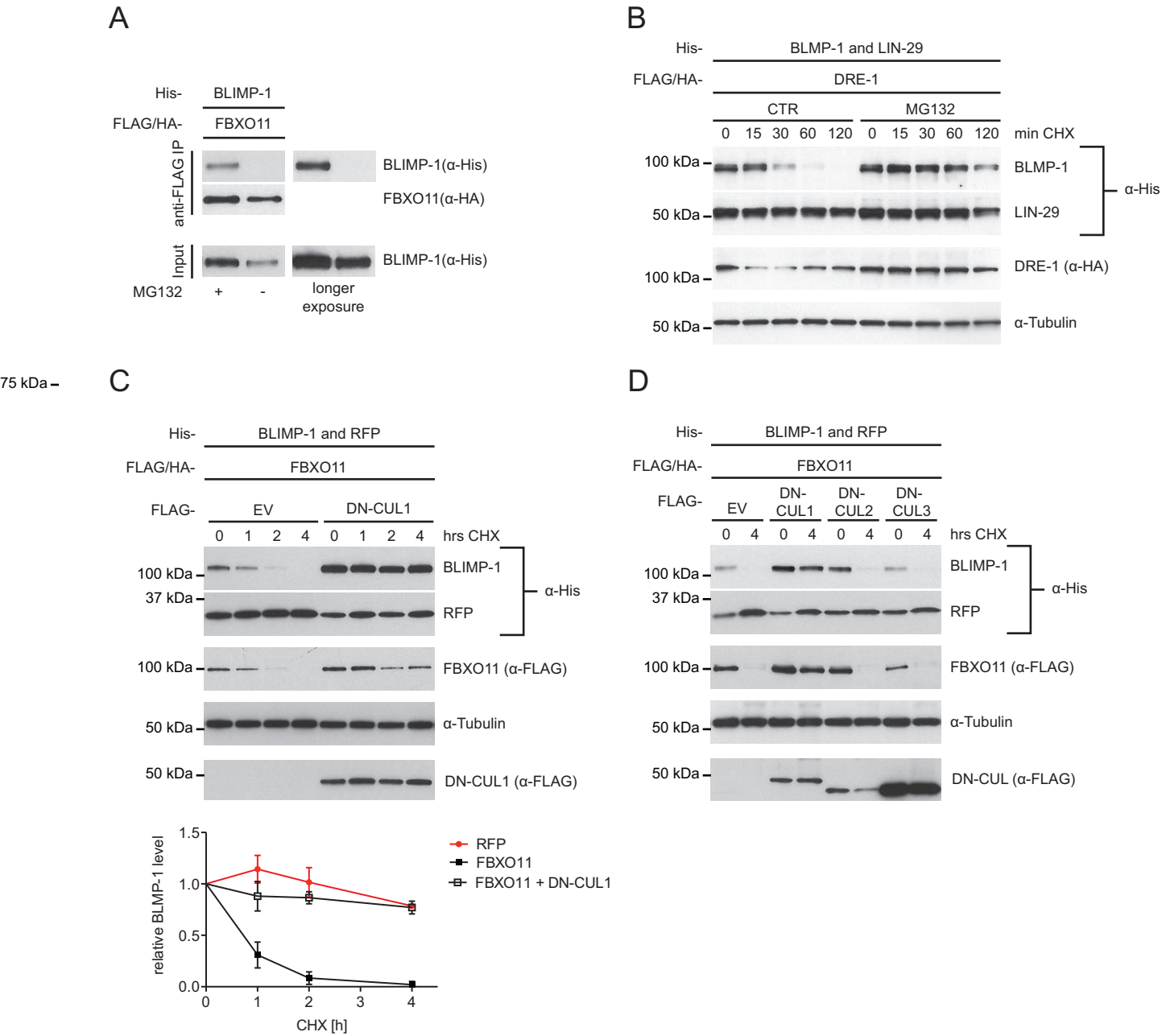

Figure S5 (related to Figure 7)

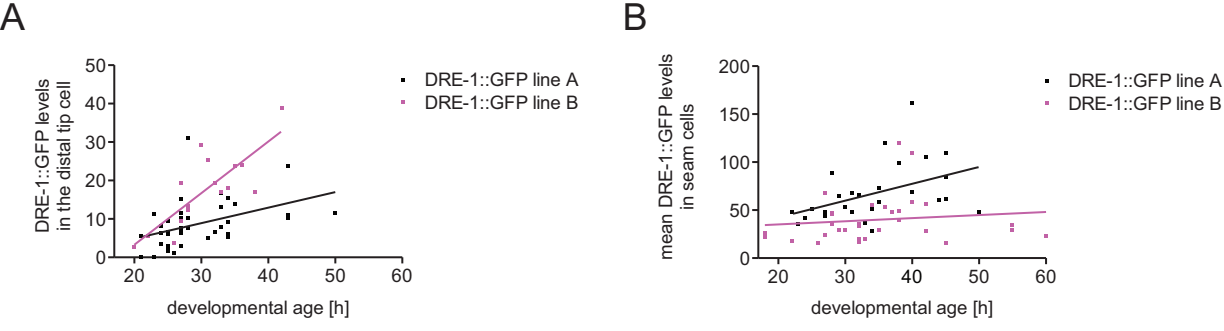

Table S1

	seam cell fusion % of worms / % of seam cells exhibiting fusion		**seam cell number ± SD**	
	L3	**L4**	**L4**	**d1A**
WT	0/0 (>50)	100/100 (21)	15.9 ± 0.45 (20)	16 ± 0.35 (17)
blmp-1(tm548)	0/0 (30)	100/100 (21)	16 ± 0.77 (21)	16.1 ± 1.15 (18)

EXTENDED EXPERIMENTAL PROCEDURES

Plasmid Construction

cDNAs for human *FBXO11*, *FBXO10*, *FBXO5*, *PRDM1*, *C. elegans dre-1*, *blmp-1, lin-29* and *Discosoma sp*. DsRed1-derived mRFP (Campbell et al., 2002) were PCR amplified with specific primers from commercially available cDNA-clones (OpenBiosystems/Thermo Scientific) or public repository plasmids (Addgene or Harvard PlasmID) and subcloned into plasmids derived from pcDNA3.1- (Invitrogen) carrying either a N-terminal 6xHis- or FLAG-HA-tag (RGS6xHis-pcDNA3.1- and FLAG-HA-pcDNA3.1-) and driving expression through the cytomegalovirus promoter. To generate RGS6xHis-pcDNA3.1- and FLAG-HA-pcDNA3.1- the following DNA oligonucleotides were subcloned into the *Nhe* I and *Xba* I sites of pcDNA3.1- using DNA-oligos (RGS6xHis: GCTAGCCACCATGAGAGGATCGCATCACCATCACCATCACGGGCCCTCTAGA; FLAG-HA: GCTAGCCACCATGGACTACAAAGACGATGACGATAAAGGGGGCGGTG GAGGTTACCCATACGATGTTCCAGATTACGCTGGTGGAGGTGGAGGTTCTAGA). The latter was only achieved after point mutation to generate a "FLAG – 5xGly – HA – 5xGly – tag", of FLAG- and the HA-tag. DN-Cullins were purchased from Addgene (15818-15820, (Jin et al., 2005)) All primer and plasmid information is available upon request.

qRT-PCR

Synchronized worms were collected in QIAzol (QIAGEN) and frozen in liquid nitrogen. Total RNA was prepared by RNeasy Mini kit (QIAGEN) and cDNA was subsequently generated by iScript cDNA Synthesis Kit (BioRad). qRT-PCR was performed with Power SYBR Green master mix (Applied Biosystems) on a ViiA 7 Real-Time PCR System (Applied Biosystems). Four technical replicates were performed in each reaction and *ama-1* served as internal control. Primer sequences are as listed below.

NGS Data Analysis

As input we had three biological replicates per sample with a library size in the range of 41-47 million reads. Sequences were trimmed at both ends with the FASTA/Q Trimmer of the FASTX-Toolkit (http://hannonlab.cshl.edu/fastx_toolkit by Hannon Lab), and then preprocessed reads were mapped to the genome with tophat2 (v2.0.7) (Kim et al., 2013) allowing only unique mapping. On average 96.1% of the reads could be aligned. Subsequently, differential gene expression analysis was performed with cuffdiff, which is part of the cufflinks package (v2.0.2) (Trapnell et al., 2010). Genes with a FPKM value >0.5 in at least one of the N2 and *blmp-1* samples were considered expressed. Those with a q-value <0.05 and fold change >±1.5 were classified as differentially expressed.

qRT-PCR primers

Gene	Primer	Sequence (5'-3')
blmp-1	fwd	ATCTTCCACACCGCCATCA
	rev	TCGCACCTGACGCTGAAAC
nas-36	fwd	CAAATGTATGGGCAGATTGGG
	rev	GGGCACGCTTTCAAATTACAG
bed-3	fwd	GCATGTTGGAAAGATTCGTGG
	rev	GGCAGCTTGTTCAATAGTTGG
wrt-2	fwd	TGCATACGCCGATCATATTCC
	rev	CAGTCCATCCGAAGCATTTTG
ptr-8	fwd	CGGCAGAAAATTCAGTCTAATCC
	rev	TCCCATTGCTTAACTGTCTTCG
col-7	fwd	CGGAATTGTGGTATTTGGAGC
	rev	CATCCTGGTTTATCATTGAGTTCC
col-124	fwd	GACTTTCTCCACCATTGCAG
	rev	GGGATACGGTTGACTTGAGAG
col-91	fwd	CGAGACTATGGAAACTTTTGACG
	rev	GAGCTTGACAGTCTGGAAGAG
ama-1	fwd	GGATGGAATGTGGGTTGAGA
	rev	CGGATTCTTGAATTTCGCGC

Strain List

N2 (Bristol)

AA426: *dre-1(dh99)V*

AA3091: *blmp-1(tm548)I*

A2601: *dre-1(dh99)V; blmp-1(tm548)I*

SU93: *jcIs1IV [ajm-1::gfp; unc-29(+); rol-6(su1006)]*

AA820: *dre-1(dh99)V; jcIs1IV*

AA2557: *blmp-1(tm548)I; jcIs1IV*

AA2666: *dre-1(dh99)V; blmp-1(tm548)I; jcIs1IV*

AA3175: *hbl-1(ve18)X; jcIs1IV*

AA832: *lin-42(n1089)II; jcIs1IV*

AA3141: *sop-2(bx91)II; jcIs1IV*

AA3242: *mab-10(e1248)II; jcIs1IV*

JR667: *unc-119(e2498::Tc1)III; wIs51[scm::gfp; unc-119(+)]*

AA2558: *blmp-1(tm548)I; wIs51*

AA3200: *mab-10(e1248)II; wIs51*

EM723: *sop-2(bx91)II; him-5(e1490)V*

MT7626: *let-7(n2853ts)X*

RG559: *hbl-1(ve18)X*

MT2257: *lin-42(n1089)II*

AA528: *dre-1(dh99)V; daf-12(rh61rh411)X*

AA885: *lin-29(n546)II; daf-12(rh61rh411)X*

AA619: *dre-1(dh99)V; lin-29(n546)II*

CB3518: *mab-10(e1248)II; him-5(e1490)V*.

AA2734: *unc-119(ed3)III; wgIs109 [blmp-1p::ORF::gfp::3xFLAG; unc-119(+)],* (Sarov et al., 2012)

AA2602: *blmp-1(tm548)I; wgIs109 [blmp-1p::ORF::gfp::3xFLAG; unc-119(+)]*

OP356: *unc-119(ed3) III; wgIs356[nhr-25::TY1::EGFP::3xFLAG; unc-119(+)]*

AA2881: *dhIs876 [dre-1p::gfp::orf 3'UTR; coel::RFP] (integrated dhEx452* (Fielenbach et al., 2007)*)*

DR1572: *daf-2(e1368)*III

CB1372: *daf-7(e1372)*III

AA2863: *daf-9(dh6)*X

SUPPLEMENTAL REFERENCES

Campbell, R.E., Tour, O., Palmer, A.E., Steinbach, P.A., Baird, G.S., Zacharias, D.A., and Tsien, R.Y. (2002). A monomeric red fluorescent protein. Proc Natl Acad Sci USA *99*, 7877–7882.

Fielenbach, N., Guardavaccaro, D., Neubert, K., Chan, T., Li, D., Feng, Q., Hutter, H., Pagano, M., and Antebi, A. (2007). DRE-1: An Evolutionarily Conserved F Box Protein that Regulates C. elegans Developmental Age. Dev Cell *12*, 443–455.

Jin, J., Ang, X.L., Shirogane, T., and Wade Harper, J. (2005). Identification of substrates for F-box proteins. Meth. Enzymol. *399*, 287–309.

Kim, D., Pertea, G., Trapnell, C., Pimentel, H., Kelley, R., and Salzberg, S.L. (2013). TopHat2: accurate alignment of transcriptomes in the presence of insertions, deletions and gene fusions. Genome Biol. *14*, R36.

Sarov, M., Murray, J.I., Schanze, K., Pozniakovski, A., Niu, W., Angermann, K., Hasse, S., Rupprecht, M., Vinis, E., Tinney, M., et al. (2012). A Genome-Scale Resource for In Vivo Tag-Based Protein Function Exploration in C. elegans. Cell *150*, 855–866.

Trapnell, C., Williams, B.A., Pertea, G., Mortazavi, A., Kwan, G., van Baren, M.J., Salzberg, S.L., Wold, B.J., and Pachter, L. (2010). Transcript assembly and quantification by RNA-Seq reveals unannotated transcripts and isoform switching during cell differentiation. Nat. Biotechnol. *28*, 511–515.